

When F_1 Fails: Granularity-Aware Evaluation for Dialogue Topic Segmentation

Michael Coen
 Independent Researcher
 mhcoen@alum.mit.edu

Preprint. Under review.

Abstract

Dialogue topic segmentation supports summarization, retrieval, memory management, and conversational continuity. Despite decades of prior work, evaluation practice in dialogue topic segmentation remains dominated by strict boundary matching and F_1 -based metrics, even as modern large language model (LLM) based conversational systems increasingly rely on segmentation to manage conversation history beyond the model’s fixed context window, where unstructured context accumulation degrades efficiency and coherence.

This paper introduces an evaluation perspective for dialogue topic segmentation that reports boundary density and segment alignment diagnostics (purity and coverage) alongside window-tolerant F_1 (W- F_1). By explicitly controlling boundary density through separating boundary scoring from boundary selection, we evaluate segmentation quality across density regimes rather than at a single operating point. Through cross-dataset empirical evaluation, we show that reported performance differences across dialogue segmentation benchmarks are often not driven by boundary placement quality alone; under common evaluation protocols, annotation granularity mismatch and sparse boundary labels can dominate these differences.

We evaluate multiple, structurally distinct dialogue segmentation strategies across eight dialogue datasets spanning task-oriented, open-domain, meeting-style, and synthetic interactions. Across these settings, we observe that boundary-based metrics are strongly coupled to boundary density, with threshold sweeps producing larger W- F_1 changes than switching between structurally distinct methods. These findings support viewing topic segmentation as a granularity selection problem rather than as the prediction of a single correct boundary set, and motivate separating boundary scoring from boundary selection as an algorithmic formulation for analyzing and tuning segmentation behavior under varying annotation granularities.

1 Introduction

Dialogue topic segmentation is commonly framed as identifying points in a conversation where “the subject changes.” This framing is appealingly simple. It is also incorrect. Topic change is often gradual, topic structure is often nested, and both depend on perspective.

Despite this, many dialogue segmentation benchmarks treat annotated boundaries as objective ground truth and evaluate systems using strict boundary matching and F_1 -based metrics [van Rijsbergen \[1979\]](#). These metrics collapse distinct failure modes into a single number. Small boundary shifts are often harmless when the goal is coherent topic blocks, while missing or adding a few boundaries can be catastrophic if boundaries drive downstream actions such as summarizing or dropping earlier turns. As we show in this paper, these effects are tightly coupled to segmentation granularity and boundary density, which are left implicit by standard boundary-based metrics.

A central difficulty is that segmentation granularity is latent in standard evaluation. Most benchmarks compare systems at a single operating point (i.e., a set of fixed thresholds or selection

settings), even though the number of boundaries produced varies across methods and datasets without explicit control. As a result, boundary-based metrics often reflect alignment in boundary *density* rather than boundary placement quality. To make granularity explicit, this work separates boundary scoring from boundary selection and evaluates performance across boundary densities rather than at a single threshold.

This paper addresses that mismatch by reframing what gets reported and what gets optimized. The evaluation objective in this paper jointly reports (i) window-tolerant F1 (W-F1), (ii) boundary density, and (iii) segment alignment diagnostics (purity and coverage). An accompanying algorithmic contribution separates boundary scoring from boundary selection, making boundary density explicit and controllable. Together, these contributions distinguish detection failures from granularity mismatches (i.e., discrepancies between the segmentation resolution at which boundaries are produced and that implied by the annotation scheme) and explain why a single global threshold fails to transfer across datasets.

We distinguish between two notions that are often conflated in boundary-based evaluation. *Boundary placement alignment* refers to whether predicted boundaries occur at the same locations as gold boundaries (within a tolerance window), which is the intended target of metrics such as F1 and W-F1. By contrast, *boundary density alignment* refers only to whether the number of predicted boundaries matches the number implied by the annotation scheme. We refer to this implicit granularity level as the annotation *regime* (e.g., coarse thematic divisions versus finer chapter- or subtopic-level segmentation), independent of which structural segmentation markers (e.g., chapters, sections, turns) are used to realize those boundaries. *Segmentation granularity* is a modeling- and selection-level property, referring to the resolution at which topic boundaries are produced. It determines boundary density through the boundary selection rule, sometimes implicitly, and thereby strongly influences boundary-based metrics.

A single-number boundary F1 can conflate two distinct factors: (i) localization (whether predicted boundaries fall near annotated topic transitions), and (ii) segmentation granularity (how many boundaries are produced overall). When the granularity of predicted segmentations differs from that implied by the annotation scheme, apparent F1 gains can arise primarily from matching the number of boundaries rather than from improved boundary placement at a matched resolution. To make this distinction explicit, we report complementary diagnostics that separately quantify boundary localization, boundary density alignment, and gold-relative segment alignment alongside tolerant boundary accuracy scores; formal definitions are given in Section 6.

Standard boundary-based evaluation implicitly assumes that, once boundary density is controlled, differences in F1 or W-F1 primarily reflect differences in boundary placement quality rather than thresholding or selection behavior. A central empirical finding of this work is that boundary-based evaluation metrics can be dominated by segmentation granularity induced by boundary selection, rather than by boundary detection quality. In particular, for a fixed scoring model, sweeping the boundary selection threshold produces larger changes in W-F1 than switching between structurally distinct segmentation methods, a pattern made explicit by density-quality curves in Section 7 (Figure 1). As a result, leaderboard-style comparisons that report only a single operating point can conflate method improvements with shifts in boundary density.

Although we do not introduce a new neural architecture for boundary scoring, the proposed separation of boundary scoring and boundary selection motivates alternative ways of reasoning about the construction, tuning, and evaluation of segmentation models under varying annotation granularities.

1. We show that boundary-based metrics (including F1 and W-F1) can be dominated by boundary density alignment: even non-semantic baselines achieve competitive scores when their output density matches the gold annotation.
2. We propose a composite evaluation objective that reports boundary density and purity/coverage alongside W-F1, exposing failure modes hidden by standard boundary metrics.

3. We demonstrate, via density-quality curves, that sweeping boundary selection thresholds for a fixed scoring model produces substantially larger changes in W-F1 and Coverage than switching between segmentation methods, making granularity mismatch explicit.
4. We show that a separation between boundary scoring and boundary selection is necessary to treat boundary density as a controllable variable rather than an incidental consequence of threshold tuning.

1.1 Motivation: Conversational Memory in AI Chat Systems

Large language model (LLM) based chat systems operate under finite context windows, which require practical systems to manage conversational history explicitly. As conversations grow longer, earlier turns must be dropped, summarized, or selectively retrieved. Topic segmentation decisions therefore directly determine which portions of prior dialogue are preserved, compressed, or reintroduced.

Importantly, this challenge does not disappear as context windows grow larger. Unstructured accumulation of earlier dialogue increases computational cost and dilutes relevance, reducing the model’s ability to focus on salient information. Effective conversational systems therefore require explicit structure over dialogue history rather than unbounded context expansion Liu et al. [2024a].

In this setting, topic segmentation functions as a memory control mechanism rather than a purely linguistic task. Poor segmentation can cause relevant context to be discarded prematurely or irrelevant context to be retained, leading to degraded long-horizon coherence and unstable behavior across turns (e.g., [Scclar et al., 2024, Razavi et al., 2025]). The lack of robust long-horizon memory remains an open challenge for current LLM-based systems, particularly in conversations spanning multiple sessions, motivating careful attention to segmentation decisions and their evaluation.

This work is motivated by the development of *Episodic*, a conversational memory system that organizes dialogue into topic-structured representations to support persistent interactions with LLM-based assistants Coen [2025]. Within such systems, boundary placement governs summarization, context selection, and context reintegration, making segmentation granularity a first-order systems design decision rather than an evaluation detail. In *Episodic*, topic segmentation interacts with neural modules for context selection, compression of accumulated history, response generation, critique, and synthesis.

Motivating observation from Episodic In early prototyping of *Episodic*, modest changes to boundary-selection parameters (and thus boundary density) produced immediately visible changes in the context assembled for the LLM and in the resulting assistant responses, even when tolerant boundary F1 changed little. Increasing density produced shorter context chunks used for LLM conditioning, which truncated cross-turn dependencies and yielded incomplete summaries. Decreasing density, by contrast, produced coarser context units that reduced resolution around topic transitions and, in some cases, suppressed boundary evidence to the point that topic transitions were not detected at all.

This effect is expected because segmentation directly determines the units selected for context reintegration (and, when needed, summarization), thereby changing the conditioning input presented within the finite context window. This effect was compounded in multi-session settings. Maintaining topic continuity required concatenating multiple same-topic segments drawn from temporally distinct conversations. Higher density amplified fragmentation, while lower density increased topic mixing. These observations motivated treating boundary density as an explicit control variable and reporting purity/coverage to distinguish within-gold refinement from cross-gold mixing and fragmentation.¹

¹We do not report a separate downstream evaluation here; this paper focuses on the evaluation and diagnostic methodology motivated by these observations.

2 Background and Related Work

Topic segmentation has a long history in text processing, with evaluation practice, dataset design, and granularity assumptions evolving somewhat independently. We organize prior work along these three dimensions.

2.1 Boundary-Based Evaluation Metrics

Topic segmentation evaluation has historically centered on boundary alignment. Early metrics such as P_k Beeferman et al. [1999] penalize segmentations where predicted and reference boundaries fall in different segments under a sliding window. WindowDiff Pevzner and Hearst [2002] refines this approach to address known biases in P_k . Both metrics are typically computed against a single reference segmentation and measure deviation from that reference, even though multiple segmentations (and granularities) can be defensible [Fournier and Inkpen, 2012, Fournier, 2013]. More recent dialogue segmentation work has largely adopted precision, recall, and exact-match F_1 computed over boundary positions Liu et al. [2024b]. These boundary-only scores likewise treat the available annotation as the evaluation target; when annotation granularity varies across datasets or differs from system behavior, they can yield misleading comparisons.

Beyond window-based and exact-match boundary scores A substantial line of work in *text segmentation evaluation* argues that (1) strict boundary matching over-penalizes near misses, and (2) window-based metrics such as P_k and WindowDiff introduce task- and parameter-dependent biases, motivating edit-distance and confusion-matrix-based alternatives. Fournier and Inkpen [2012] propose *segmentation similarity* (S), an edit-distance-based similarity that is symmetric (does not privilege a single “true” reference) and supports evaluation against multiply-coded corpora. Fournier [2013] extend this direction with *boundary edit distance* and *boundary similarity* (B), yielding a principled way to obtain boundary-level IR-style quantities (precision/recall/ F) while awarding graded credit for near misses. Relatedly, Scaiano and Inkpen [2012] derive a boundary confusion matrix from WindowDiff-style windows (WinPR), separating false positives from false negatives while retaining tunable near-miss sensitivity. For corpora with multiple annotators or where segmentation is treated as a *unitizing* task, agreement measures that jointly align and score units (e.g., γ) provide an alternative to single-reference evaluation [Mathet et al., 2015].

2.2 Dialogue Segmentation Datasets

Dialogue topic segmentation introduces complexity beyond written text due to turn-taking, discourse phenomena, and gradual topic transitions. Several benchmarks have emerged with distinct annotation philosophies. DialSeg711 Liu et al. [2022] and SuperDialseg Liu et al. [2023] provide densely annotated dialogue corpora, while TIAGE Sun et al. [2020] annotates topic boundaries in task-oriented dialogue with sparser labels tied to task structure. MultiWOZ Budzianowski et al. [2018] provides domain annotations that can be interpreted as coarse topic boundaries. Open-domain and semi-structured datasets such as DailyDialog Li et al. [2020], Taskmaster Byrne et al. [2019], Topical-Chat Gopalakrishnan et al. [2019], and QMSum Zhong et al. [2021] reflect further variation in how *topic-like* structure is operationalized, including domain/section labels or derived boundary heuristics rather than explicit topic-boundary annotation. This diversity in annotation intent produces systematic differences in boundary density across datasets—differences that standard boundary scores do not distinguish from detection quality.

2.3 Segmentation Granularity

Classic segmentation methods such as TextTiling Hearst [1997] and Choi-style benchmarks Choi [2000] established the paradigm of predicting a single boundary set evaluated against gold annotations.

More recent work has also reframed segmentation as supervised boundary prediction on large automatically-derived corpora (e.g., Wikipedia section boundaries), typically evaluated with boundary- and window-based metrics [Koshorek et al., 2018]. Across these settings, research has refined scoring models and architectures, but the assumption that a single “correct” granularity exists has remained largely unexamined. Prior work rarely treats segmentation granularity as a first-class, controllable variable: boundary density is typically a side effect of threshold tuning rather than an explicit design choice, and evaluation protocols do not distinguish between detection failures (placing boundaries at incorrect locations) and granularity mismatches (producing a different number of boundaries than the annotation scheme implies). This paper addresses that gap by separating boundary scoring from boundary selection and proposing evaluation criteria that make granularity effects explicit.

Multiple valid granularities and weakly-identified boundaries Empirical studies of human segmentation consistently emphasize that topical structure is only weakly identified by surface form: topic change is gradual, the task is under-defined, and annotators operate at different granularities. In a large-scale topical segmentation study, Kazantseva and Szpakowicz [2012] report low overall inter-annotator agreement but substantially higher agreement on a subset of *prominent* breaks, motivating prominence-weighted evaluation. More broadly, discourse segmentation work notes weak consensus on what the relevant units and criteria should be, even when humans can be reliable under a fixed criterion [Passonneau and Litman, 1997]. These findings support the premise of this paper: benchmark boundary sets reflect one operational granularity among many, so boundary-only scores can conflate boundary *localization* with *granularity/density alignment*.

3 Problem Setting

Topic boundaries are not intrinsic properties of conversations; they are defined relative to a chosen segmentation granularity, which reflects task requirements and user or annotator preferences about where topical divisions should be made. A model that produces fine-grained discourse-phase boundaries can be operationally reasonable yet score poorly against a dataset that annotates only coarse task transitions. Conversely, a model tuned to sparse labels may suppress meaningful subtopic structure in order to match the annotated boundary density.

In contrast, this paper treats topic segmentation as two separate operations:

1. **Boundary scoring:** assign a score to each candidate boundary position.
2. **Boundary selection:** choose which candidates become output boundaries, controlling boundary density and spacing.

Collapsing these operations makes boundary density an accidental byproduct of threshold tuning. Our baseline experiments confirm that this produces systematically misleading results: the effect is demonstrated in Section 6.5. Figure 2 (§ 8.1) provides a concrete worked example of this granularity mismatch.

4 Datasets

We evaluated multiple, structurally distinct dialogue segmentation strategies across eight dialogue datasets spanning diverse dialogue regimes. The purpose of cross-dataset evaluation here is not only to compare performance, but to expose how annotation philosophy and boundary density interact with evaluation metrics.

Task-oriented dialogue datasets include SuperDialseg Liu et al. [2023], DialSeg711 Liu et al. [2022], TIAGE Sun et al. [2020], and MultiWOZ Budzianowski et al. [2018]. Open-domain and semi-structured datasets include DailyDialog (synthetic concatenations) Li et al. [2020], Taskmaster Byrne

et al. [2019], Topical-Chat Gopalakrishnan et al. [2019], and QMSum Zhong et al. [2021]. Several datasets provide sparse boundaries by design or annotate boundaries with intent (e.g., summarization units), which is precisely the setting where exact-match F1 becomes fragile. Together, these datasets span sparse, medium, and dense annotation regimes, providing a testbed for evaluating segmentation behavior under annotation granularity shift.

We refer to the SuperDialseg dataset as *SuperSeg* throughout. Separately, we denote the periodic oracle *baseline family* as *Oracle-Periodic (Every-N)*.

Converting the datasets to a common canonical format is described in Appendix D.

5 Methodology

This section operationalizes the separation between boundary scoring and boundary selection introduced in Section 3 for empirical evaluation.

Experimental scope The experiments reported in Sections 6 and 7 intentionally evaluate only the neural boundary scoring component under static threshold+gap selection. Episodic, as deployed, is a hybrid system in which neural boundary scores are complemented by additional online signals, including embedding-drift-based change detection used by the commitment policy described in Appendix F. These auxiliary signals are not used in the main experiments and are held out deliberately to isolate the behavior of boundary-based evaluation metrics under controlled changes in boundary density. Accordingly, the performance tables and density-quality curves should be interpreted as diagnostics of scoring and selection behavior under controlled boundary densities.

5.1 Topic Segmentation Algorithm

Given a dialogue consisting of messages m_1, \dots, m_T , we define candidate boundary positions $i \in \{1, \dots, T-1\}$ between adjacent messages.

Selection rule family Boundary selection operates over candidate positions after scoring, and is independent of the specific scoring model used. All boundary selection methods used in this work instantiate a common selection primitive: a boundary at position i is committed iff (i) its accumulated evidence $e_i(t)$ exceeds a threshold $\tau(t)$, and (ii) it is separated by at least g messages from any previously committed boundary. The *static* selection rule used in the main experiments is the special case where $e_i(t) = s_i$ for all t at which position i is evaluated (no temporal accumulation) and $\tau(t) = \tau$ is fixed. The *adaptive* selection rule illustrated in Figure 3 and discussed in Section 9.1 generalizes this primitive by defining (a) an online evidence accumulator $e_i(t)$ and (b) a time-varying threshold $\tau(t)$, adjusted to enforce a target boundary rate relative to the number of candidate positions processed (see Appendix F for a complete formal specification).

Selection hyperparameters and transparency Boundary density is controlled entirely by the boundary selection rule through the threshold τ and minimum spacing parameter g . In all experiments reported in this paper, g is fixed to a single global value across all datasets, and τ is fixed globally after temperature calibration. Neither parameter is tuned per dataset, per split, or on held-out validation data to match gold boundary counts or to optimize any evaluation metric. As a result, variation in boundary density across datasets reflects differences in annotation granularity rather than dataset-specific hyperparameter adjustment. This choice is intentional: per-dataset tuning of g or τ would partially obscure the granularity effects this work aims to expose.

Boundary scoring For each candidate position i , the scorer computes a real-valued score $s_i \in \mathbb{R}$, where larger values indicate stronger evidence of a topic boundary. Scores are computed using a

window-vs-window comparison: a window of turns preceding position i is compared against a window of turns following i , rather than relying on the adjacent message pair alone.

Boundary selection The scorer ranks candidates; boundary selection determines which become final boundaries. In online settings (i.e., incremental, decision-time selection as dialogue unfolds), selection may accumulate evidence over time before committing to a boundary. This separation decouples final segmentation granularity from the scorer’s behavior.

Static boundary selection rule (used in experiments) In our experiments, boundary selection reduces to a static selection rule based on thresholding with minimum spacing.

1. Select all candidate positions i such that $s_i \geq \tau$.
2. Enforce a minimum spacing g via greedy non-maximum suppression: candidates are processed in descending score order, and a candidate i is accepted only if no previously accepted boundary lies within g positions.

The resulting set of topic boundaries is $B \subseteq \{1, \dots, T - 1\}$.

Scope. For Figure 3, we allow the threshold τ to vary over time (logged as `min_evidence`, the running evidence threshold used by the selection rule); all other aspects of the selection rule remain unchanged. During evidence accumulation, candidate scores are evaluated against a fixed pre-change reference. Freezing both the pre-boundary context and the boundary-adjacent anchor turn ensures that the selection rule measures persistence of topic departure rather than repeated detection of the same topic transition.

Threshold sweeps for density–quality curves To construct density–quality curves (Section 7.1), we sweep the selection threshold τ over a fixed linear grid while holding the spacing parameter g constant at $g = 3$. Specifically, τ is swept linearly over the interval $[0.05, 0.95]$ in increments of 0.05, yielding 19 operating points per method. At each value of τ , boundary selection is performed using the same static selection rule, and boundary density, W-F1, purity, and coverage are recomputed. No other parameters are varied during the sweep.

Selection hyperparameters (reported values) All main experimental results reported in Sections 6–7 use a fixed minimum spacing of $g = 3$ messages and a fixed global threshold of $\tau = 0.50$ applied to temperature-calibrated scores. These values are held constant across all datasets, splits, and runs.

5.2 Scoring Model Architecture

The boundary scoring model is a fine-tuned DistilBERT-based binary classifier. For each candidate boundary position i , the model encodes a left context window and a right context window around i using the input format `[CLS] pre-window [SEP] post-window [SEP]`. Unless otherwise specified, the scoring model uses a symmetric local context window of $k=4$ utterances before and after each candidate boundary (total window size 9), truncated at dialogue boundaries when insufficient context is available. The final hidden state of the `[CLS]` token is passed through a linear projection layer to produce a scalar score $s_i \in \mathbb{R}$ representing boundary confidence.

The model is trained using binary cross-entropy loss on boundary labels. No architectural modifications beyond the classification head are introduced; the purpose of this implementation is to provide a stable scoring signal rather than to optimize segmentation performance.

5.3 Training Procedure

We train the scoring model in three stages, summarized in Table 1:

Stage 1: Synthetic Pretraining. We construct synthetic splice examples by concatenating real dialogue segments and labeling the splice point as a boundary. The synthetic splice corpus is constructed exclusively from training splits of the dialogue datasets listed in Table 1, ensuring no overlap with validation or test data. We remove boundary-local artifacts (e.g., greetings) to prevent spurious cues, and we evaluate a negative control set of single-segment examples to verify that the model does not hallucinate boundaries. While some synthetic splice points may join semantically related segments, this introduces conservative label noise that discourages hallucinated boundaries rather than inducing spurious segmentation.

Stage 2: Supervised Fine-Tuning on Benchmarks. We next perform supervised fine-tuning on benchmark datasets. Table 8 summarizes performance over five epochs.

Stage 3: Calibration and Final Evaluation. We apply temperature scaling to calibrate score magnitudes by optimizing a single scalar temperature $T > 0$ on a held-out validation set (minimizing negative log-likelihood). This operation rescales the logits used to produce boundary scores, improving score comparability and numerical stability across runs. After calibration, the resulting model is evaluated without further tuning on the test splits of all datasets.

Importantly, temperature calibration rescales *evidence* but does not determine how many boundaries are produced. Boundary density is controlled exclusively by the selection rule (thresholding and spacing), not by temperature. While changing T shifts the score distribution, it does not encode a target boundary rate and cannot, by itself, enforce consistent segmentation granularity across datasets. Calibration therefore improves the interpretability of scores but does not resolve granularity mismatch, which remains a decision-level issue handled by explicit boundary selection.

Reproducibility The reference implementation for this work is available in the Episodic repository at <https://github.com/mhcoen/episodic>. The `paper/` directory within this repository contains the LaTeX source for the paper, experiment configuration files, and evaluation scripts required to reproduce the reported results.

Data availability All datasets used in this study are publicly available from their original sources and are cited in the paper. Due to licensing restrictions, we do not redistribute raw dialogue data. Instead, the repository provides scripts to download, preprocess, and evaluate each dataset in accordance with its original distribution terms.

Protocol clarification Stage 2 supervised fine-tuning is performed exclusively on the *training splits* of SuperSeg and TIAGE; no other benchmark datasets are used for supervised learning. Stage 3 temperature calibration learns a single global temperature using a held-out *validation split* of SuperSeg only.

6 Evaluation Metrics

We evaluate dialogue topic segmentation using metrics that separately characterize boundary placement, boundary density, and gold-relative segment alignment. This separation is necessary to distinguish boundary localization errors from granularity mismatch and segment-level structural effects that standard boundary-based scores conflate. Formal mathematical definitions are provided in Appendices A–C; the metrics are described here at an operational level to support interpretation of the empirical results.

Stage	Purpose	Datasets	Split
Stage 1	Synthetic pretraining	Synthetic splice corpus	Train / val
Stage 2	Supervised fine-tuning	SuperSeg, TIAGE	Train only
Stage 3a	Temperature calibration	SuperSeg	Validation only
Stage 3b	Final evaluation	All 8 datasets	Test only

Table 1: Training, calibration, and evaluation protocol by stage. Stage 2 supervised fine-tuning uses only the training splits of SuperSeg and TIAGE to expose the scorer to both dense and sparse annotation regimes. Temperature calibration learns a single global temperature on a held-out validation split of SuperSeg. Stage 3 evaluation is performed on test splits only, including both datasets seen during training and datasets held out entirely from training and calibration.

F_1 over boundaries We treat topic segmentation as predicting a set of boundary indices $P_d \subseteq \{1, \dots, T_d - 1\}$ and compare against gold boundaries $G_d \subseteq \{1, \dots, T_d - 1\}$. We compute precision = $|P_d \cap G_d|/|P_d|$, recall = $|P_d \cap G_d|/|G_d|$, and F_1 as the usual harmonic mean. For brevity, we refer to this metric simply as F_1 throughout.

Evaluation objectives Dialogue topic segmentation evaluation must distinguish between three conceptually distinct properties: (i) boundary placement near annotated topic transitions, (ii) alignment between predicted and annotated boundary density (annotation regime), and (iii) internal coherence of resulting segments with respect to the gold segmentation. Standard boundary-based metrics collapse these properties into a single score. The evaluation framework used here reports them separately.

6.1 Window-tolerant boundary accuracy (W-F1)

What W-F1 measures W-F1 measures boundary placement accuracy under a fixed tolerance window. A predicted boundary is counted as correct if it lies within a small window around a gold boundary, rather than requiring an exact index match. This makes W-F1 robust to small positional shifts that are often operationally irrelevant. The variant used here adopts a window-coverage convention, under which multiple predicted boundaries may fall within the tolerance window of a single gold boundary and be counted as correct. Formally, W-F1 is computed from dialogue-level precision and recall defined over boundary sets P_d and G_d using a tolerance window $\pm w$ (see Appendix A for the full definition).

Interpretation and rationale This window-coverage design is intentionally recall-favoring. Precision under W-F1 should therefore be interpreted as the fraction of predicted boundaries that fall near annotated topic transitions, rather than as a one-to-one measure of boundary set agreement. We adopt this convention to decouple boundary localization from boundary count, allowing W-F1 to serve as a diagnostic of whether boundaries are placed near annotated transitions. For this reason, W-F1 must be interpreted in conjunction with separate measures that account for boundary density and segment structure.

Relation to one-to-one tolerant matching (not used) A common alternative is *one-to-one* tolerant matching, where each gold boundary may be matched to at most one prediction within $\pm w$. Under this convention, additional predicted boundaries near the same gold transition are counted as false positives, making precision sensitive to boundary count as well as boundary location. Because this couples localization with boundary density, one-to-one tolerant matching is not well suited to isolating boundary placement behavior under varying segmentation granularities.

Robustness to tolerant matching variants Although our primary analysis uses many-to-one window-coverage matching, we additionally evaluate a standard one-to-one tolerant matching variant (maximum bipartite matching within the same tolerance window; see Appendix G to verify that the density-driven effects reported in this paper are not an artifact of the matching convention. Across both datasets, the resulting density-quality curves remain qualitatively unchanged (Figure 4).

Scope of the definition This W-F1 definition should not be assumed equivalent to other window-tolerant F1 variants in prior work. A complete, reimplementable definition—including matching rules, empty-set handling, and aggregation—is given in Appendix A.

6.2 Boundary density (BOR)

Boundary Over-segmentation Ratio (BOR) measures the number of predicted boundaries relative to the number of gold boundaries. Although termed the boundary oversegmentation ratio, BOR is used here as a general boundary density ratio: values greater than 1 indicate oversegmentation relative to gold, while values less than 1 indicate undersegmentation. Formally, BOR is defined as the ratio $|P_d|/|G_d|$, computed per dialogue and aggregated across dialogues.

Boundary-based accuracy metrics alone cannot distinguish boundary placement quality from boundary density alignment. A system can achieve high W-F1 simply by matching the annotation boundary count, even with non-semantic boundary placement. BOR exposes this effect directly by making boundary density explicit.

6.3 Segment alignment: purity and coverage

Definition and rationale Purity and coverage measure how well predicted segments align with the gold segmentation, independent of exact boundary placement. Purity asks whether each predicted segment draws most of its turns from a single gold segment (limited cross-gold mixing), while coverage asks whether each gold segment is largely captured by a single predicted segment (limited fragmentation). Together, these measures distinguish between adding boundaries that primarily refine gold segments and boundaries that cut across or fragment them irregularly.

Aggregation We report turn-weighted (micro) purity and coverage, computed per dialogue and then aggregated across dialogues. Unweighted segment-level (macro) variants are not monotone under refinement and are therefore not used. Formal definitions and aggregation rules are given in Appendix B.

6.4 Failure-mode interpretation

The three reported diagnostics—W-F1, BOR, and purity/coverage—must be interpreted jointly. W-F1 captures boundary misalignment under window-based matching. BOR ($|P|/|G|$) exposes systematic over- or under-segmentation. Purity and coverage are *gold-relative segment alignment* diagnostics: they measure how predicted and gold segments relate structurally (limited cross-gold mixing versus fragmentation/subdivision), and should not be interpreted as independent semantic coherence estimates.

Table 2 summarizes the characteristic regimes that arise under different combinations of boundary accuracy, boundary density, and purity/coverage.

The baseline experiments in the following section illustrate several of these regimes.

6.5 Baselines

We evaluate simple non-semantic baselines to illustrate how boundary density alone can dominate boundary-based evaluation. These baselines provide reference points for interpreting density-driven

F1/W-F1	BOR	Purity/Coverage	Interpretation
High	≈ 1	High (both)	Calibrated (aligned granularity)
High	$\gg 1$	High purity	Oversegmentation (fine-grained, gold-consistent)
Low	$\gg 1$	High purity	Granularity mismatch (not necessarily noisy)
Low	< 1	High coverage	Undersegmentation (coarser-than-gold)
Low	≈ 1	Low (both)	Detection failure (misplaced/noisy)

Table 2: **Failure modes of boundary-based evaluation.** Distinct segmentation behaviors can yield similar boundary accuracy scores unless boundary density (BOR) and purity/coverage are reported.

Baseline	Dataset	W-F1	BOR	Purity	Coverage
No-boundary	DialSeg711	0.000	0.00	0.438	1.000
	SuperSeg	0.113	0.00	0.568	1.000
	TIAGE	0.140	0.00	0.541	1.000
Oracle-periodic Every- N	DialSeg711 ($N = 4$)	0.639	0.97	0.812	0.823
	SuperSeg ($N = 2$)	0.623	1.10	0.830	0.775
	TIAGE ($N = 3$)	0.610	0.97	0.849	0.774
Oracle-density Random (BOR=1)	DialSeg711	0.528	1.00	0.839	0.833
	SuperSeg	0.678	1.00	0.883	0.884
	TIAGE	0.664	1.00	0.873	0.869

Table 3: **Baseline diagnostic statistics relative to gold annotations.** Oracle-density baselines match gold boundary counts by construction.

effects independent of semantic boundary placement.

We consider three classes of baselines: (i) a no-boundary baseline, (ii) periodic segmentation baselines, and (iii) oracle-density random baselines. Oracle-density baselines explicitly use gold boundary counts and are therefore not deployable; they are included solely to expose the sensitivity of boundary metrics to density alignment.

Purity and coverage are reported here as diagnostic statistics rather than as standalone evaluation objectives. In particular, increasing boundary density tends to increase purity and decrease coverage regardless of semantic validity.

These results instantiate several regimes from Table 2, including density-matched baselines achieving competitive W-F1 despite lacking semantic grounding.

7 Results

This section evaluates the proposed separation between boundary scoring and boundary selection under differing annotation granularity. The results below instantiate multiple failure modes summarized in Table 2, including for previously published methods re-evaluated under the same framework.

7.1 Granularity as a Controlled Variable

To isolate the effect of segmentation granularity from boundary ranking quality, we evaluate each method across a range of boundary densities by sweeping the boundary selection threshold while holding the scoring model fixed. This produces *density-quality curves* that explicitly expose how boundary-based metrics vary as a function of output density rather than at a single operating point.

Figure 1 presents these curves for DialSeg711 and SuperSeg, illustrating two qualitatively distinct annotation regimes.

Interpreting density–quality curves Each density–quality curve in Figure 1 traces a *single* segmentation method under different boundary-selection thresholds. Moving horizontally along a curve changes only the *number* of output boundaries, as measured by BOR, while holding the underlying scorer fixed. Vertical separation between curves at a matched BOR therefore reflects differences in boundary *ranking* quality, whereas horizontal movement along a curve reflects changes in segmentation granularity induced by selection. If boundary-based metrics primarily measured boundary detection quality, methods would be cleanly separated vertically at matched BOR; instead, the dominant variation is typically along the BOR axis, indicating strong coupling between W-F1/Coverage and boundary density.

Dataset-dependent density sensitivity Figure 1 highlights a sharp contrast between SuperSeg and DialSeg711. On SuperSeg, W-F1 is maximized near $\text{BOR} \approx 1$ and degrades rapidly under under- or over-segmentation, indicating that evaluation strongly enforces the annotation boundary density. On DialSeg711, by contrast, W-F1 exhibits a broad plateau across BOR, and oversegmentation is comparatively weakly penalized. This contrast implies that identical boundary-based metrics can encode substantially different effective granularity assumptions across datasets.

Across both datasets, the proposed neural scorer is consistently higher than baselines at matched BOR, particularly in the conservative regime ($\text{BOR} < 1$), indicating improved boundary ranking.

7.2 External Methods Under Granularity-Aware Evaluation

To assess whether the granularity effects identified in this work are specific to our scoring model or reflect broader evaluation behavior, we re-evaluated a representative subset of published dialogue segmentation methods under the proposed granularity-aware framework. The selected methods include simple baselines (random and periodic segmentation), a classical unsupervised approach (TextTiling), and a coherence-based model (CSM). All methods were evaluated using the same boundary canonicalization and metrics as in previous sections.

External-method re-evaluations: scope and controls All external-method results use the same boundary representation and tolerance window w , and all metrics (F1, W-F1, BOR, purity, coverage) are computed by a single implementation under a shared canonicalization (Appendix D). We therefore interpret Table 4 as follows: under our canonicalization and operating-point protocol, apparent single-number method differences largely coincide with BOR shifts.

These re-evaluations are not intended as reproductions of published leaderboard numbers. Reported scores can depend on underspecified or inconsistent details across papers, including preprocessing (tokenization/turn handling and boundary canonicalization), dataset splits, and operating-point selection; code and tuning procedures are also not always available. A reproduction-oriented setup would therefore entangle boundary density with these factors.

Instead, we evaluate all methods within a single canonicalized pipeline with controlled density sweeps, so that BOR is an explicit, comparable axis across methods. This design isolates the effect of boundary density by holding canonicalization and selection behavior fixed across methods. The audit protocol and canonicalization details are provided in Appendix H.

All single-point results reported below correspond to individual operating points along the density–quality curves shown in Figure 1.

Several patterns in Table 4 align with the failure modes summarized in Table 2. Simple periodic segmentation achieves competitive boundary accuracy when its output density aligns with the gold annotation ($\text{BOR} \approx 1$), despite lacking semantic grounding. Classical methods such as TextTiling exhibit recall-dominated behavior with elevated BOR, yielding high purity alongside aggressive

DialSeg711 and SuperSeg: Density–Quality Regime Plots with 95% CIs

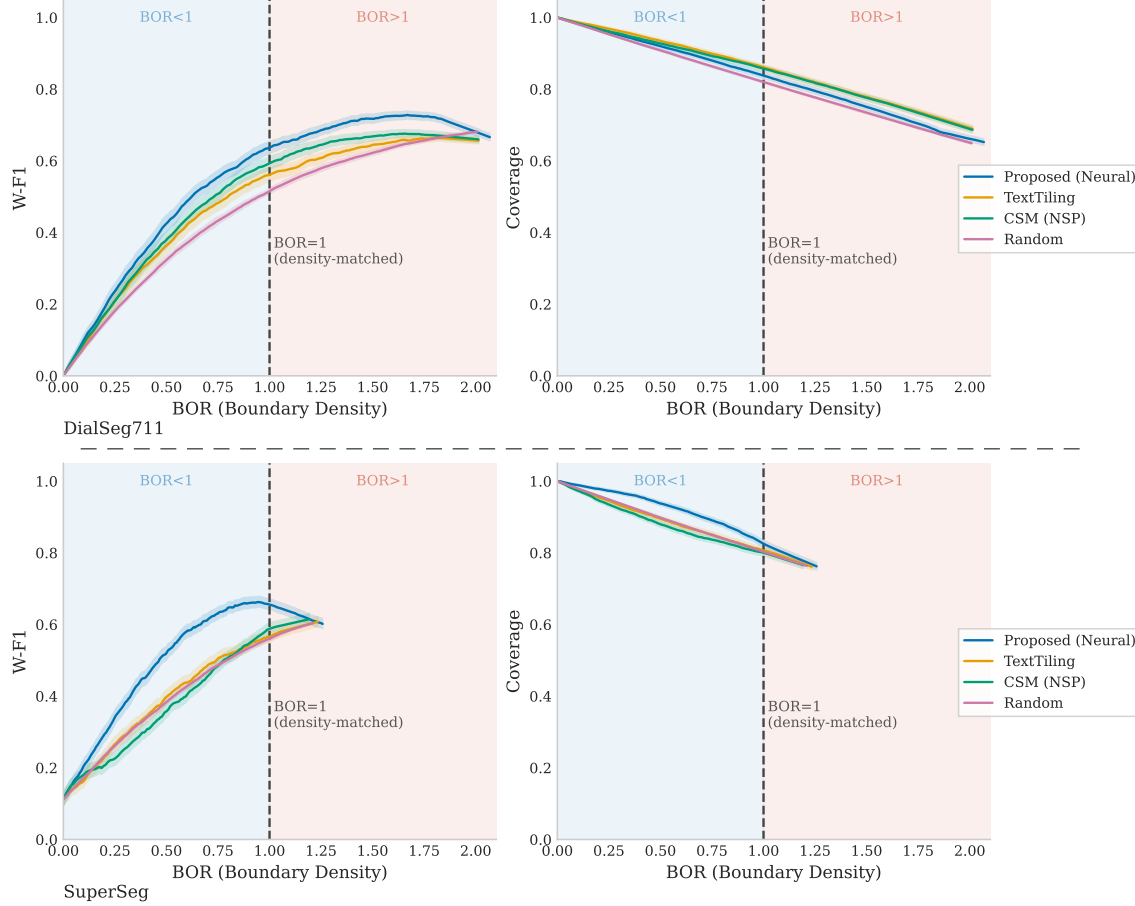


Figure 1: **Density–quality curves for DialSeg711 and SuperSeg.** Each curve varies the boundary-selection threshold for a fixed scoring model. Horizontal movement (changing boundary density) produces substantially larger changes in W-F1 and Coverage than vertical separation between methods, including for the proposed neural scorer. SuperSeg exhibits a comparatively narrow optimum near $\text{BOR} \approx 1$, while DialSeg711 tolerates a broader range of boundary densities, indicating dataset-dependent coupling between boundary-based metrics and annotation granularity. Shaded regions surrounding each curve indicate 95% dialogue-level bootstrap confidence intervals; curves are shown over the full realized BOR range for each dataset under the same threshold sweep. Results reflect the Episodic neural boundary scorer evaluated under static selection and are diagnostic of evaluation behavior rather than full deployed system performance.

oversegmentation. Notably, the same method (CSM) occupies different density regimes across datasets, indicating that apparent performance differences often reflect density mismatch rather than improved boundary detection.

For clarity, and following the failure taxonomy in Table 2, we categorize the results in Table 4 as conservative ($\text{BOR} < 1$), balanced ($\text{BOR} \approx 1$), or aggressive ($\text{BOR} \gg 1$), as summarized in Table 5.

Targeted audit of runnable SuperDialseg leaderboard comparisons We audit three runnable comparisons drawn from the SuperDialseg benchmark leaderboard by re-evaluating the corresponding publicly available implementations under our canonicalized pipeline and metrics (same tolerance

Method	Dataset	W-F1	BOR	F1	Purity	Coverage
TextTiling	DialSeg711	0.648	1.88	0.550	0.968	0.746
CSM	DialSeg711	0.412	0.64	0.373	0.749	0.921
Random	DialSeg711	0.267	0.55	0.098	0.711	0.890
Oracle-Periodic	DialSeg711	0.483	1.00	0.211	0.806	0.809
TextTiling	TIAGE	0.612	2.04	0.445	0.949	0.693
CSM	TIAGE	0.615	3.97	0.346	0.976	0.454
Random	TIAGE	0.256	0.33	0.121	0.697	0.921
Oracle-Periodic	TIAGE	0.620	1.00	0.300	0.832	0.838

Table 4: **External dialogue segmentation methods re-evaluated under the proposed granularity-aware framework.** Boundary density (BOR) varies substantially across methods and datasets, producing distinct density regimes despite comparable boundary accuracy scores.

Method	Dataset	Density Regime
TextTiling	DialSeg711	Aggressive ($\text{BOR} \gg 1$)
CSM	DialSeg711	Conservative ($\text{BOR} < 1$)
Random	DialSeg711	Conservative ($\text{BOR} < 1$)
Oracle-Periodic	DialSeg711	Balanced ($\text{BOR} \approx 1$)
TextTiling	TIAGE	Aggressive ($\text{BOR} \gg 1$)
CSM	TIAGE	Aggressive ($\text{BOR} \gg 1$)
Random	TIAGE	Conservative ($\text{BOR} < 1$)
Oracle-Periodic	TIAGE	Balanced ($\text{BOR} \approx 1$)

Table 5: Density regimes under the proposed failure taxonomy, derived from BOR thresholds.

window w as above). Although the comparisons originate from the SuperDialseg leaderboard, the audited methods are evaluated here on DialSeg711 and TIAGE (both included in SuperDialseg’s evaluation suite). In all three cases, the reported F1/W-F1 deltas coincide with higher boundary density (positive ΔBOR), consistent with the density-regime effect analyzed above.

These three comparisons exhaust the set of SuperDialseg leaderboard entries that we can reproduce from publicly available, deterministic implementations without retraining and without proprietary or deprecated APIs. We therefore restrict the audit to methods with runnable code under these constraints. In particular, the InstructGPT baseline reported in SuperDialseg uses `text-davinci-003`, which has since been deprecated and is no longer available, so we do not include it here.

Concrete example of a likely confounded comparison Table 6 provides a direct illustration of how published boundary-metric “improvements” can be driven by density regime shifts rather than improved boundary placement. For example, on DialSeg711, the comparison *TextTiling vs. CSM* shows a substantial increase in W-F1 ($\Delta\text{W-F1} = +0.220$) accompanied by a large increase in boundary density ($\Delta\text{BOR} = +2.13$), moving from a conservative regime ($\text{BOR} < 1$) to an aggressive regime ($\text{BOR} \gg 1$). Under the failure taxonomy in Table 2, this pattern is consistent with recall-dominated oversegmentation: higher tolerant boundary scores arise from emitting many more boundaries, not necessarily from more accurate boundary localization at a matched granularity.

7.3 Stage 1: Synthetic Pretraining on Splice Boundaries

This stage isolates whether the scoring model can learn a meaningful boundary signal in a controlled setting, independent of annotation noise. Performance here reflects the model’s ability to distinguish

Comparison	Dataset	$\Delta F1$	$\Delta W-F1$ [95% CI]	ΔBOR [95% CI]	Density Shift
TT vs. CSM	DialSeg711	+0.135	+0.220 [0.202, 0.237]	+2.13 [2.07, 2.18]	Conservative \rightarrow Aggressive
TT vs. CSM	TIAGE	+0.128	+0.219 [0.155, 0.283]	+1.26 [1.11, 1.44]	Aggressive \rightarrow More Aggressive
TT vs. Oracle-P	DialSeg711	+0.277	+0.132 [0.114, 0.150]	+1.69 [1.64, 1.74]	Balanced \rightarrow Aggressive

Table 6: **Pairwise audit of runnable SuperDialseg leaderboard comparisons with 95% dialogue-level bootstrap confidence intervals.** TT denotes TextTiling and Oracle-P is the Oracle-Periodic (Every- N) baseline. Positive Δ indicates higher values for the first-listed method. Arrows denote relative changes in boundary density from the second-listed method to the first-listed method. Regime labels follow Table 2.

Epoch	F1	W-F1	BOR	Mean score	Neg. Ctrl.
1	0.265	0.420	0.31	0.007	0.000
2	0.453	0.688	0.67	0.009	0.032
3	0.489	0.733	0.87	0.010	—

Table 7: **Stage 1 synthetic pretraining on splice boundaries.** Mean $|score|$ denotes the mean boundary score magnitude $\mathbb{E}[|s_i|]$ on the validation set and serves as a diagnostic for score collapse. Negative control (Neg. Ctrl.) reports the predicted boundary rate on single-segment dialogues, which should be near zero; it was not rerun for epoch 3, as the model had already passed this sanity check at epoch 2.

genuine topic transitions from non-boundaries before exposure to real dialogue benchmarks. Table 7 summarizes boundary-level behavior during this phase.

While some synthetic splice points may join semantically related segments, this introduces conservative label noise that discourages hallucinated boundaries rather than inducing spurious segmentation.

7.4 Stage 2: Supervised Fine-Tuning on Benchmarks

This stage performs supervised fine-tuning to align the scoring model with human annotation conventions on in-distribution datasets. The key question is whether boundary density stabilizes without degrading boundary ranking quality. Table 8 reports performance over five fine-tuning epochs. Supervised fine-tuning is therefore in-distribution only for SuperSeg and TIAGE. Results on these datasets in Stage 3 reflect performance after exposure to their annotation regimes, whereas results on all other datasets reflect cross-dataset generalization under annotation-granularity shift.

7.5 Stage 3: Final Test with Calibration

Final test protocol Stage 3 evaluation is performed on the *test splits* of all eight datasets. This includes datasets seen during Stage 2 training (SuperSeg, TIAGE) as well as datasets not used for supervised training or calibration (DialSeg711, MultiWOZ, DailyDialog, Taskmaster, Topical-Chat, QMSum). No dataset-specific thresholds, temperatures, or selection parameters are tuned at this stage.

Epoch	Overall F1	W-F1	BOR	SuperSeg F1/BOR	TIAGE F1/BOR
1	0.778	0.833	1.11	0.788 / 1.13	0.197 / 0.24
2	0.819	0.850	1.23	0.830 / 1.25	0.352 / 0.86
3	0.840	0.865	1.13	0.852 / 1.14	0.337 / 0.82
4	0.848	0.875	1.08	0.862 / 1.08	0.322 / 0.78
5	0.843	0.872	1.04	0.857 / 1.05	0.311 / 0.84

Table 8: **Stage 2 supervised fine-tuning on benchmark datasets.** Boundary density converges toward annotated density ($BOR \approx 1$) on datasets seen during training, while W-F1 remains high.

Dataset	W-F1	BOR	F1	Pred./Gold Boundaries
DialSeg711	0.767	2.53	0.434	5167/2042
SuperSeg	0.584	0.81	0.609	2376/2923
TIAGE	0.512	0.76	0.368	157/207

Table 9: **Stage 3 final test results.** Boundary density (BOR) is reported alongside boundary accuracy to distinguish granularity mismatch from detection failure.

This stage evaluates generalization under distribution shift, where annotation granularity differs from the training regime. Here, the focus is not peak F1 but the interaction between boundary ranking, boundary density, and calibration.

Final test results are shown in Table 9, which reports evaluation metrics for a representative subset of three datasets spanning sparse, medium, and dense annotation regimes; results on the remaining datasets follow the same qualitative pattern.

Calibration. We learned a single global temperature of $T = 0.976$ for this run. In practice, temperature scaling modestly improves score calibration and threshold stability, but it does not eliminate cross-dataset threshold non-transfer: differences in annotation granularity continue to dominate the relationship between score thresholds and boundary density.

Complete Stage 3 calibrated results for all eight datasets are reported in Appendix E.

8 Gold-Relative Segment Alignment Under Granularity Mismatch

These diagnostics are essential for interpreting boundary-based metrics under granularity mismatch. In particular, they distinguish between two qualitatively different outcomes that exact-match metrics conflate: (1) segmentations that introduce additional boundaries that predominantly *subdivide gold segments* (high purity), and (2) segmentations that place boundaries in ways that *mix* turns from multiple gold segments or yield unstable purity/coverage under matched density.

As shown in Table 10, the proposed model maintains high purity across datasets even when its boundary density exceeds that of the gold annotation. Relative to random baselines with matched density ($BOR = 1$), this indicates that the additional boundaries are model-induced and predominantly subdivide gold segments, rather than reflecting density-matched random placement. In contrast, baseline methods that match gold density achieve competitive boundary scores but exhibit lower or unstable purity/coverage, showing that density alignment alone does not guarantee usable segmentation.

Taken together, these results suggest that the scorer shares the annotators’ inductive bias: it recovers many annotated boundaries and, when producing finer segmentations ($BOR > 1$), predominantly subdivides within gold segments rather than cutting across them. We treat this as alignment with the gold topic partition, not as an independent guarantee of semantic coherence.

Dataset	W-F1	BOR	Purity	Coverage	F1
DialSeg711	0.767	2.53	0.962	0.651	0.434
SuperSeg	0.584	0.81	0.847	0.915	0.609
TIAGE	0.512	0.76	0.785	0.896	0.368

Table 10: **Gold-relative segment alignment diagnostics for the proposed model.** High purity with elevated BOR indicates fine-grained subdivision that largely preserves the gold partition; high coverage with reduced BOR indicates coarser-than-gold segmentation. Purity and coverage are gold-relative diagnostics and should not be interpreted as independent semantic coherence estimates. Both patterns reflect granularity mismatch rather than boundary detection failure.

8.1 Worked Example

Figure 2 isolates the granularity-mismatch regime: the model predicts additional boundaries that are not annotated in the (coarser) gold segmentation. Under strict precision/recall, these extra predicted boundaries are treated as false positives, reducing F_1 even in settings where purity/coverage indicate limited cross-gold mixing (cf. Table 10).

This example makes the failure mode concrete. The additional predicted boundaries reflect finer-grained discourse transitions according to the model, but they occur within a gold span and are therefore penalized by exact-match evaluation. As a result, F_1 can drop substantially despite correct identification of the major topic transition. The dominant discrepancy is thus one of boundary density and segmentation granularity rather than gross boundary misplacement, motivating evaluation that distinguishes granularity mismatch from detection failure.

9 Discussion

The results demonstrate that boundary-based accuracy metrics conflate segmentation quality with boundary density alignment when annotation granularity varies. In particular, the apparent competitiveness of oracle-density baselines in Table 3 should not be interpreted as modeling capability, but as evidence that boundary accuracy metrics reward density alignment rather than transferable boundary detection. Random and periodic strategies achieve competitive W-F1 and purity scores when their output boundary density is matched to the gold annotation, despite lacking any semantic grounding. In contrast, the proposed model yields substantially higher segment purity on datasets with coarse annotations, at the cost of elevated BOR, indicating limited cross-topic mixing relative to gold spans rather than detection failure.

Across datasets, we observe two stable annotation regimes: sparse gold (few annotated boundaries per dialogue) and dense gold (many annotated boundaries per dialogue).

When gold annotations are relatively uniform (e.g., DialSeg711), granularity errors concentrate in a small subset of atypical dialogues. In this setting, emitting additional boundaries is often beneficial, and W-F1 continues to improve under moderate oversegmentation.

When gold annotations are highly variable (e.g., SuperSeg), granularity mismatch is distributed more evenly across dialogues. Here, performance is tightly coupled to the annotated density, and W-F1 is locally flat near the gold boundary rate.

These regime-specific behaviors explain the distinct shapes of the density-quality curves and show that boundary-based metrics entangle density alignment with segmentation quality in different ways across datasets.

Figure 1 reinforces this point by showing that the variation in W-F1 induced by sweeping the boundary selection threshold for a fixed scoring model (moving along a curve) is substantially larger than the variation observed between segmentation methods at a matched boundary density. *This behavior is contrary to the standard evaluation assumption that boundary-based metrics primarily*

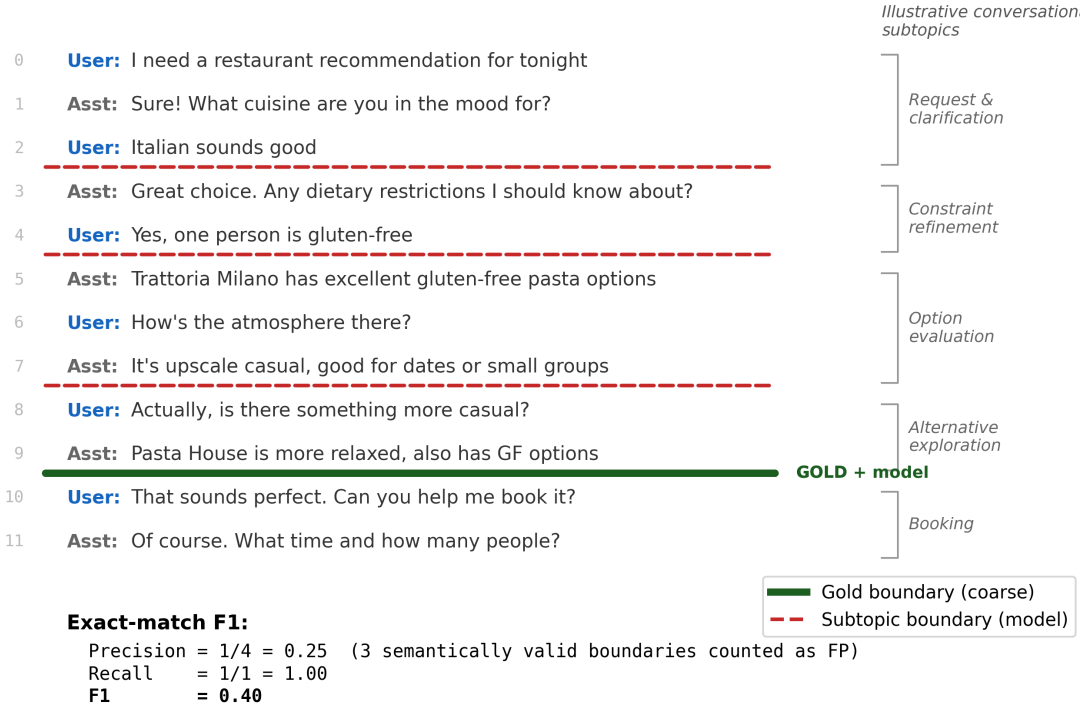


Figure 2: **Granularity mismatch in dialogue topic segmentation.** Gold annotations mark a single coarse topic boundary (browsing → booking), while the model predicts multiple additional boundaries associated with finer-grained discourse transitions. Under exact-match evaluation, three additional predicted boundaries are counted as false positives, yielding $F_1=0.40$ despite correct identification of the coarse transition. The discrepancy reflects a mismatch in boundary density and segmentation granularity rather than gross boundary detection error.

reflect boundary placement quality once density is controlled. We intentionally do not prescribe a universal target BOR, as any such prescription would reintroduce a single “correct” granularity that this work argues does not exist.

Importantly, this evaluation failure is not model-specific under these benchmarks and evaluation protocols: any method whose output boundary density is tuned to match the gold annotation can achieve competitive F1 and W-F1 scores, as demonstrated by the non-semantic baselines in Table 3. We do not attempt a comprehensive retrospective survey of published claims across all leaderboards and datasets; instead, we provide targeted, runnable audits (Table 6) that concretely demonstrate how apparent boundary-metric gains can arise from substantial shifts in boundary density regimes. Adding more segmentation models does not resolve this problem; it only illustrates it further.

Prior work and common usage patterns of classical change-detection and drift-based strategies are consistent with this conclusion. Under standard boundary-based evaluation protocols, such strategies are typically recall-driven: they increase boundary density to improve tolerant boundary metrics such as W-F1, frequently yielding boundary oversegmentation ratios well above 1.0. The proposed evaluation objective makes this trade-off explicit: methods with higher W-F1 but elevated BOR are identified as oversegmenting, while more conservative scorers exhibit lower boundary accuracy but better density control.

At a conceptual level, three qualitatively distinct boundary-density regimes can be distinguished:

- **Conservative strategies**, which undersegment and produce $\text{BOR} < 1$, yielding lower recall but stable coverage.

- **Balanced strategies**, which achieve $\text{BOR} \approx 1$ with high purity and coverage, yielding segmentation aligned with the annotation granularity.
- **Aggressive strategies**, which substantially increase boundary density ($\text{BOR} \gg 1$) to maximize recall and tolerant boundary scores, resulting in recall-dominated detection rather than calibrated segmentation.

To confirm that granularity effects are not specific to our scorer, we evaluated CSM [Xing and Carenini \[2021\]](#), a published coherence-based segmentation model, under the same framework. CSM operates in the conservative regime ($\text{BOR} = 0.64$), producing fewer boundaries than the gold annotation. Its low strict F1 (0.373) reflects low recall rather than incoherent segmentation: coverage remains high (0.921), indicating that predicted segments are valid but coarser than the reference. This demonstrates that the granularity–F1 interaction identified here generalizes across structurally distinct segmentation methods.

In practice, selection thresholds should therefore be chosen based on intended downstream use rather than optimized solely to match a particular annotation density. Boundary density metrics such as BOR provide a simple diagnostic for tuning selection behavior without retraining the scoring model.

Practical guidance for choosing boundary density The appropriate boundary selection behavior depends on how segmentation outputs are used downstream. Based on the empirical results in this study, we offer the following high-level guidance:

- **Summarization and context truncation.** When topic boundaries trigger summarization or removal of prior turns, missing a major boundary can be more harmful than introducing extra minor boundaries. Conservative selection is therefore preferable: a lower boundary density ($\text{BOR} < 1$) reduces the risk of prematurely discarding relevant context, even if some distinct topics are merged.
- **Retrieval and navigation.** For applications that rely on topic boundaries to index or retrieve relevant conversation segments, finer-grained segmentation can be beneficial. In such settings, semantic coherence is an engineering objective of the topic segmentation algorithm itself rather than a quantity directly evaluated here. When boundary density increases ($\text{BOR} > 1$) but purity remains high, the additional boundaries predominantly reflect within-gold subdivision rather than cross-gold cuts, yielding finer-grained retrieval units consistent with the gold topic partition.
- **Exploratory analysis and annotation.** When segmentation is used for qualitative analysis, annotation support, or exploratory inspection, fine-grained boundaries are often desirable. In such settings, boundary density may substantially exceed that of existing annotations, and evaluation should emphasize purity/coverage over exact boundary alignment.

These guidelines reinforce the central claim of this paper: boundary density is not an intrinsic property of a conversation, but a design choice that should be tuned to application requirements rather than optimized to match a given annotation scheme. This dependence on selection behavior motivates treating boundary selection as a distinct, explicit step.

9.1 Boundary Selection as a Separate Step

Scope. All offline evaluations (Sections 6–7) use the static threshold+gap rule over one-shot scores (§5.1). The adaptive evidence-accumulating controller (Appendix F) is used only for the control experiment in this subsection (Figure 3).

Figure 3 illustrates the consequence of separating scoring from selection: different scoring granularities produce substantially different candidate boundary rates, yet an explicit selection

rule enforces stable output boundary distributions that are invariant to the scorer’s granularity. Crucially, this invariance does not arise from score rescaling or post-hoc normalization. The scoring function is unchanged; identical output distributions emerge solely from the selection mechanism’s evidence accumulation and adaptive thresholding behavior. This behavior illustrates that separating scoring from selection enables boundary density to be controlled independently of scoring granularity, motivating its treatment as a design parameter rather than an evaluation artifact. A fully specified and reimplementable version of this adaptive controller is given in Appendix F.

9.2 Computational Cost

Boundary selection is computationally negligible: it operates on a vector of scores and applies thresholding and minimum spacing. Boundary scoring dominates cost because it requires running the neural model over candidate positions (window-vs-window inputs around each position). The separation therefore has practical value in deployed systems: selection can be retuned per dataset or application without recomputing scores, while recomputing scores requires model inference. Evidence accumulation within online boundary selection is likewise lightweight relative to scoring, since it reuses the fixed-reference scores and maintains only decision state.

9.3 On Dataset Choice and External Validity

Public dialogue datasets are necessarily imperfect proxies for real human–AI interactions. While several conversational AI datasets have been released, we are not aware of any publicly available corpus of long, open-ended human–AI conversations with turn-level topic boundary annotations suitable for evaluating segmentation granularity. Our claims therefore concern evaluation behavior under heterogeneous annotation schemes rather than direct modeling of user behavior. The consistency of failure modes across diverse datasets indicates that these effects arise from evaluation practice rather than dataset-specific artifacts.

Human–LLM chat data and annotation availability Few large-scale corpora of human–LLM interaction are publicly available, and none currently include turn-level topic boundary annotations suitable for segmentation evaluation. WildChat [Zhao et al. \[2024\]](#), for example, contains over one million authentic user–assistant exchanges but is released without discourse- or topic-level segmentation labels. Nevertheless, such data exhibit strong initiative asymmetries: users introduce goals and direct topic shifts, while assistant turns are reactive responses constrained by the preceding query. This asymmetry is well established in studies of institutional and task-oriented interaction [Drew and Heritage \[1992\]](#) and has been shown to shape discourse segmentation under mixed-initiative conditions [Grosz and Sidner \[1990\]](#). In deployed AI assistant systems, these asymmetries are typically addressed through systems-level design choices for intent tracking and context management [Chopra et al. \[2024\]](#), which operate downstream of the boundary detection problem studied here.

Given the absence of annotated human–LLM dialogue data, the present study does not model speaker-specific segmentation policies. Instead, it examines how boundary-based evaluation metrics behave under varying annotation granularities using existing human–human and task-oriented dialogue corpora with explicit topic labels. Alternative segmentation unit choices (e.g., restricting candidates to user turns only) reflect engineering considerations for deployed systems and primarily rescale the set of candidate boundary positions; they do not fundamentally alter the evaluation phenomena analyzed here, which concern the interaction between boundary density, placement quality, and segment structure relative to gold annotations. Empirical validation on annotated human–LLM data remains an important direction for future work.

10 Limitations and Future Work

This work contributes (i) an evaluation objective that makes boundary density and segment coherence explicit and (ii) a topic segmentation algorithm that separates boundary scoring from boundary selection. We do not explore alternative neural backbones or include a direct ablation comparing synthetic pretraining against training from scratch. Preliminary experiments indicate that splice-boundary pretraining primarily stabilizes early training dynamics rather than improving final performance, but a systematic ablation remains an important direction for follow-up work.

Purity and coverage are computed with respect to the same gold annotations whose granularity we argue is often mismatched to model behavior. Accordingly, these measures should not be interpreted as independent estimates of semantic coherence. Rather, they function as relative diagnostics: high purity rules out incoherent mixing of gold topics, while elevated BOR distinguishes fine-grained subdivision from boundary noise. Independent coherence measures (e.g., embedding-based similarity or human judgments) would be valuable complements, but are not required for the present goal of diagnosing evaluation failure modes under mismatched annotation granularity.

Interpretation constraint Purity and coverage should be interpreted only conditional on non-trivial boundary detection performance (e.g., W-F1 significantly greater than zero). When considered in isolation, both measures can be arbitrarily high or low for segmentations with no semantic content, including density-matched random baselines.

Statistical variability We report dialogue-level bootstrap confidence intervals for selected figures and tables (e.g., Figure 1 and Tables 3–4) to characterize variability arising from dialogue sampling under fixed model checkpoints and boundary-selection parameters. These intervals are computed by resampling dialogues and do not reflect variability across random seeds, training runs, or alternative model initializations.

We do not report multi-run or multi-seed confidence intervals or formal significance tests across independent training runs. Our primary claims concern qualitative failure modes and regime-level behavior (e.g., recall-dominated oversegmentation versus calibrated segmentation), which manifest as large and consistent shifts in boundary density and coherence that substantially exceed the within-sample bootstrap variability observed here. Multi-seed experiments indicated that run-to-run variance was small relative to these effects and did not alter the qualitative conclusions. A systematic multi-run statistical analysis remains a direction for future work.

Inter-annotator agreement (IAA) statistics could also provide additional empirical support for the claim that topic boundaries are granularity-dependent rather than objective. Several dialogue segmentation datasets report IAA in their original publications (e.g., DialSeg711 [Liu et al. \[2022\]](#), SuperSeg [Liu et al. \[2023\]](#)), often showing only moderate agreement even under controlled annotation protocols. However, these statistics are reported using heterogeneous definitions and units (e.g., boundary placement, segment overlap, or task-level agreement), making direct comparison across datasets difficult. Because the present work focuses on evaluation behavior under fixed annotation schemes rather than on the reliability of those schemes themselves, we do not reanalyze annotator agreement here. Integrating IAA into a unified analysis of granularity effects remains an important direction for future work.

Additional directions include evaluating published dialogue segmentation methods under the proposed evaluation objective to confirm that the observed granularity effects are method-agnostic, and exploring alternative boundary selection rules that adapt boundary density to application constraints rather than annotation conventions. Further study is also needed to relate boundary density preferences to specific downstream uses such as summarization, retrieval, or conversational memory. Finally, future work could replace discrete boundary representations with continuous or multi-scale topic representations (e.g., topic clouds) that better capture overlapping, gradual, or revisited conversational structure.

11 Conclusion

Dialogue topic segmentation does not admit a single ground truth. Exact boundary matching conflates detection correctness with segmentation granularity and can obscure coherent segmentation behavior under heterogeneous annotation schemes. By evaluating boundary density and purity/coverage alongside W-F1, this work provides a principled basis for diagnosing evaluation failure modes that boundary accuracy metrics alone cannot distinguish.

A central empirical finding of this work is that boundary-based metrics can be dominated by boundary density alignment rather than boundary placement quality. For example, we observe that the same published method (CSM) occupies different density regimes across datasets, a pattern consistent with differences in annotation density rather than changes in detection capability. Targeted audits of runnable SuperDialseg leaderboard comparisons further show that apparent gains in boundary accuracy frequently coincide with shifts toward more aggressive density regimes, rather than improved boundary localization at a matched granularity.

Boundary-based accuracy metrics should not be interpreted at a single operating point without accompanying density and purity/coverage. More broadly, segmentation granularity should be treated as a design choice conditioned on downstream use, not as an implicit property of a benchmark annotation scheme.

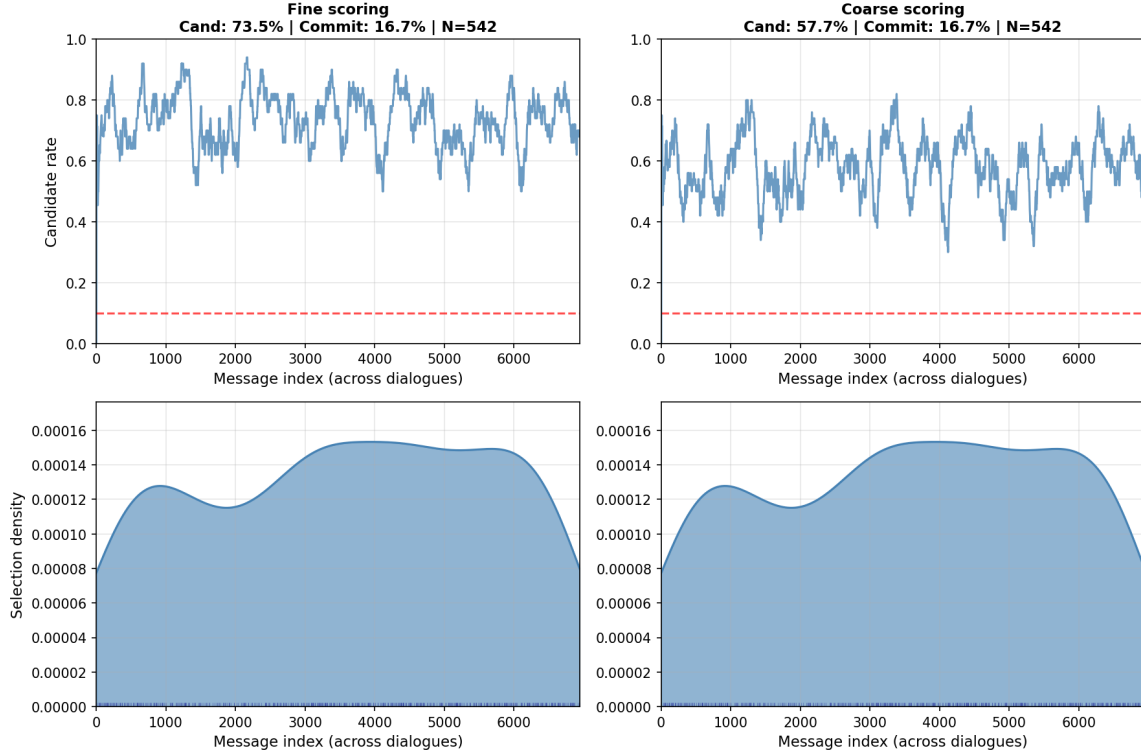


Figure 3: **Adaptive boundary selection enforces invariant boundary distributions across scoring granularities (DialSeg711).** *Top row* shows the raw candidate boundary rate produced by the same scorer under fine (left) and coarse (right) candidate thresholds, resulting in substantially different candidate frequencies (73.5% vs. 57.7%). The dashed line indicates the target selection rate specified to the controller. *Bottom row* shows the resulting distribution of selected boundaries over message index after adaptive thresholding. Despite large differences in candidate generation, adaptive selection converges to nearly identical boundary distributions and total selection counts (16.7% selection rate, $N=542$ in both cases). This invariance is not the result of score rescaling or post-hoc normalization: the underlying scoring function is unchanged, and the effect emerges from online evidence accumulation and adaptive thresholding, reflecting successful decoupling of boundary selection from boundary scoring. The adaptive selection procedure illustrated here is formally specified in Appendix F.

A Window-tolerant F1 (W-F1)

This appendix provides the formal mathematical definition of the window-tolerant F1 metric used throughout the paper. The main text remains fully interpretable without consulting this appendix.

Let a dialogue d consist of T_d turns, with gold boundary indices $G_d \subset \{1, \dots, T_d - 1\}$ and predicted boundary indices $P_d \subset \{1, \dots, T_d - 1\}$. Let $w \geq 0$ denote the tolerance window.

Window-coverage matching Define the number of window-matched predicted boundaries

$$TP_d = |\{p \in P_d : \exists g \in G_d \text{ such that } |p - g| \leq w\}|,$$

and the number of recovered gold boundaries

$$MG_d = |\{g \in G_d : \exists p \in P_d \text{ such that } |p - g| \leq w\}|.$$

Under this window-coverage convention, multiple predicted boundaries may be matched to the same gold boundary, while each gold boundary contributes at most once to recall.

Dialogue-level precision and recall Precision and recall are defined per dialogue with explicit empty-set handling:

$$\begin{aligned} \text{Prec}_d &= \begin{cases} \text{TP}_d/|P_d|, & |P_d| > 0, \\ 1, & |P_d| = 0 \wedge |G_d| = 0, \\ 0, & |P_d| = 0 \wedge |G_d| > 0, \end{cases} \\ \text{Rec}_d &= \begin{cases} \text{MG}_d/|G_d|, & |G_d| > 0, \\ 1, & |G_d| = 0 \wedge |P_d| = 0, \\ 0, & |G_d| = 0 \wedge |P_d| > 0. \end{cases} \end{aligned}$$

Dialogue-level W-F1 The window-tolerant F1 score for dialogue d is

$$\text{W-F1}_d = \begin{cases} \frac{2 \text{Prec}_d \text{Rec}_d}{\text{Prec}_d + \text{Rec}_d}, & \text{Prec}_d + \text{Rec}_d > 0, \\ 0, & \text{otherwise.} \end{cases}$$

Dataset-level aggregation Dataset-level W-F1 is computed as a macro average over dialogues:

$$\text{W-F1} = \frac{1}{|D|} \sum_{d \in D} \text{W-F1}_d.$$

Scope note This definition specifies the W-F1 variant used throughout this paper and should not be assumed equivalent to other window-tolerant F1 formulations that employ different matching or aggregation rules.

Alternative (not used): one-to-one window matching For completeness, we define a one-to-one variant that credits at most one prediction per gold boundary. Let H_d be a bipartite graph with left nodes P_d , right nodes G_d , and an edge (p, g) iff $|p - g| \leq w$. Let M_d be a maximum-cardinality matching in H_d , and define $TP_d^{1:1} := |M_d|$. Then

$$\text{Prec}_d^{1:1} = \frac{TP_d^{1:1}}{|P_d|}, \quad \text{Rec}_d^{1:1} = \frac{TP_d^{1:1}}{|G_d|},$$

with the same empty-set conventions as above, and $\text{W-F1}_d^{1:1}$ as the harmonic mean of $\text{Prec}_d^{1:1}$ and $\text{Rec}_d^{1:1}$. All results in this paper use the window-coverage definition presented here (i.e., TP_d and MG_d as defined above), not the one-to-one variant.

B Purity and Coverage

This appendix defines the purity and coverage diagnostics used to characterize gold-relative segment alignment in Section 6.

Let a dialogue d be segmented into predicted segments $P_d^{\text{seg}} = \{p_1, \dots, p_m\}$ and gold segments $G_d^{\text{seg}} = \{g_1, \dots, g_n\}$, where each segment is a contiguous span of turns and the segmentations form partitions of $\{1, \dots, T_d\}$.

For a segment $s = [a, b]$, let $|s| = b - a + 1$ denote its length in turns, and for two segments s and t define their overlap

$$|s \cap t| = \max(0, \min(b_s, b_t) - \max(a_s, a_t) + 1).$$

Segment-level purity and coverage For a predicted segment $p \in P_d^{\text{seg}}$, define its purity as

$$\text{Purity}(p) = \max_{g \in G_d^{\text{seg}}} \frac{|p \cap g|}{|p|}.$$

For a gold segment $g \in G_d^{\text{seg}}$, define its coverage as

$$\text{Coverage}(g) = \max_{p \in P_d^{\text{seg}}} \frac{|p \cap g|}{|g|}.$$

Dialogue-level micro averages Turn-weighted (micro) purity and coverage for dialogue d are

$$\text{Purity}_d = \frac{1}{T_d} \sum_{p \in P_d^{\text{seg}}} \max_{g \in G_d^{\text{seg}}} |p \cap g|,$$

$$\text{Coverage}_d = \frac{1}{T_d} \sum_{g \in G_d^{\text{seg}}} \max_{p \in P_d^{\text{seg}}} |p \cap g|.$$

Dataset-level aggregation Dataset-level purity and coverage are computed as macro averages over dialogues:

$$\text{Purity} = \frac{1}{|D|} \sum_{d \in D} \text{Purity}_d, \quad \text{Coverage} = \frac{1}{|D|} \sum_{d \in D} \text{Coverage}_d.$$

C Monotonicity Properties

This appendix formalizes monotonicity properties referenced in Section 6.

Lemma (Purity is monotone under refinement) Let P'_d be a refinement of P_d , obtained by adding predicted boundaries (i.e., splitting predicted segments). Then

$$\text{Purity}_d(P'_d, G_d) \geq \text{Purity}_d(P_d, G_d).$$

Proof It suffices to consider splitting a single predicted segment $p \in P_d$ into subsegments p_1, \dots, p_k . Let $g^* \in G_d^{\text{seg}}$ be a gold segment maximizing overlap with p . Since the p_i partition p ,

$$|p \cap g^*| = \sum_{i=1}^k |p_i \cap g^*|.$$

For each i , $\max_g |p_i \cap g| \geq |p_i \cap g^*|$. Summing over i yields a non-decreasing contribution to Purity_d , while all other segments are unchanged. \square

Dataset	Unit	Annotation $\rightarrow G_d$ rule	Filtering notes
DialSeg711	U	Segment ID change between consecutive utterances	All turns retained; indexed consecutively
SuperSeg	U	Segment ID change between consecutive utterances	All turns retained; indexed consecutively
TIAGE	U	Task/topic segment change between consecutive utterances	All turns retained; indexed consecutively
MultiWOZ	U	Domain label change between consecutive utterances	All turns retained; indexed consecutively
DailyDialog	U	Topic category change between consecutive utterances	All turns retained; indexed consecutively
Taskmaster	U	Task or subtask label change between consecutive utterances	All turns retained; indexed consecutively
Topical-Chat	U	Conversation topic change between consecutive utterances	All turns retained; indexed consecutively
QMSum	T	Section/topic boundary between adjacent speaker turns	Meeting metadata removed

Table 11: Boundary canonicalization details required to reproduce gold boundary sets G_d from each dataset. Unit codes: **U** = utterance-level boundaries between consecutive turns from either speaker; **T** = speaker-turn boundaries.

Remark (Coverage under refinement) Under the same refinement, $\text{Coverage}_d(P'_d, G_d) \leq \text{Coverage}_d(P_d, G_d)$, since splitting predicted segments cannot increase the maximum overlap with any fixed gold segment.

D Boundary canonicalization

All datasets are converted to a canonical message sequence m_1, \dots, m_T per dialogue, where each m_t corresponds to one dataset-provided utterance after filtering (below). Candidate boundary indices are the between-message positions $i \in \{1, \dots, T-1\}$.

Filtering We (i) retain all dialogue turns from both speakers (user and agent/assistant), removing only dataset-level metadata headers where present (e.g., meeting preambles in QMSum), (ii) preserve speaker role labels but do not include them in utterance text, and (iii) remove empty or whitespace-only utterances if any exist. After filtering, messages are reindexed so that all boundary indices refer to positions in the filtered sequence.

Gold boundary extraction For each dataset, we define the gold boundary set $G_d \subseteq \{1, \dots, T_d-1\}$ using the dataset’s native segment annotation as follows:

- **Datasets with segment IDs per utterance:** let ℓ_t be the segment ID for message m_t ; then $G_d = \{i : \ell_i \neq \ell_{i+1}\}$.
- **Datasets with explicit boundary markers:** let $b_t \in \{0, 1\}$ indicate that m_t starts a new segment; then $G_d = \{i : b_{i+1} = 1\}$.
- **Domain-/state-labeled datasets:** let label_t denote the dataset-provided label for message m_t ; then $G_d = \{i : \text{label}_i \neq \text{label}_{i+1}\}$.

Dataset-specific notes We provide per-dataset extraction details (file paths, fields, and filtering) in Table 11.

Dataset	W-F1	BOR	Purity	Coverage	Pred./Gold
DialSeg711	0.767	2.53	0.962	0.651	5167/2042
SuperSeg	0.584	0.81	0.847	0.915	2376/2923
TIAGE	0.512	0.76	0.785	0.896	157/207
DailyDialog	0.398	0.91	0.783	0.885	182/200
MultiWOZ	0.738	2.22	0.950	0.757	2475/1117
Taskmaster	0.288	5.23	0.955	0.565	1026/196
Topical-Chat	0.289	3.91	0.939	0.620	766/196
QMSum	0.154	17.56	0.979	0.459	3705/211

Table 12: **Stage 3 calibrated results for all eight datasets.** Metrics computed under the same calibrated Stage 3 pipeline used in Table 9, with identical model checkpoint, temperature calibration ($T = 0.976$), boundary canonicalization, and selection settings. This appendix reports a subset of diagnostics focused on boundary density and segment coherence; strict exact-match F1 is intentionally omitted because it is highly sensitive to aggregation and boundary sparsity and is not a primary diagnostic in the proposed evaluation objective.

E Full Stage 3 Calibrated Results Across All Datasets

All results reported in this appendix use the identical Stage 3 evaluation pipeline and are computed exclusively on *test splits*: a single model checkpoint after Stage 2 training, a single global temperature calibrated on the SuperSeg validation split, fixed boundary canonicalization, and fixed boundary-selection parameters. No information from any test split is used during training or calibration. The evaluation protocol follows the train/validation/test split specification summarized in Table 1.

The main text (Section 7.5) reports Stage 3 calibrated results on three representative datasets spanning sparse, medium, and dense annotation regimes. To substantiate the cross-dataset claims made in Sections 4 and 7, this appendix reports the same Stage 3 evaluation metrics for all eight datasets used in this study: DialSeg711, SuperSeg, TIAGE, MultiWOZ, DailyDialog, Taskmaster, Topical-Chat, and QMSum.

All results in Table 12 were computed using the identical Stage 3 evaluation pipeline as the main Stage 3 results (Table 9): a single globally calibrated temperature ($T = 0.976$), identical boundary canonicalization, fixed boundary selection parameters, and the evaluation definitions in Section 6.

We report window-tolerant boundary detection (W-F1 with a ± 1 message tolerance), boundary density relative to gold annotations (BOR), and segment coherence diagnostics (purity and coverage), along with predicted and gold boundary counts. Strict exact-match boundary F1 is omitted here because it is highly sensitive to aggregation choice (e.g., micro vs. macro averaging) and boundary sparsity, and it is not a primary diagnostic in the proposed evaluation objective.

F Adaptive Boundary Selection

This appendix provides a formal specification of the adaptive boundary selection mechanism referenced in Section 9.1.

Definitions and target rate Candidate boundaries correspond to between-message indices $i \in \{1, \dots, T-1\}$, where i denotes the position between messages (m_i, m_{i+1}) .

Let $C(t)$ denote the number of candidate positions processed up to time t , and let $S(t)$ denote the number of boundaries committed up to time t . The adaptive controller targets a boundary *selection rate*

$$\rho = \mathbb{E} \left[\frac{S(t)}{C(t)} \right],$$

Algorithm 1: Adaptive boundary selection

Input: target rate ρ , spacing g , window size W , step size η , initial threshold $\tau(0)$
Output: committed boundary set \mathcal{B}

$$\mathcal{B} \leftarrow \emptyset$$

Initialize counters $C \leftarrow 0$, $S \leftarrow 0$

for each time step t as messages arrive **do**

- for** each newly available candidate i **do**

 - compute frozen score s_i ; set $e_i \leftarrow 0$

- for** each active candidate i **do**

 - $e_i \leftarrow e_i + s_i$
 - $C \leftarrow C + 1$
 - if** $e_i \geq \tau(t)$ **and** $|i - b| \geq g$ for all $b \in \mathcal{B}$ **then**

 - $\mathcal{B} \leftarrow \mathcal{B} \cup \{i\}$
 - $S \leftarrow S + 1$

compute $\hat{\rho}(t)$ over last W candidates

$$\tau(t+1) \leftarrow \tau(t) + \eta(\hat{\rho}(t) - \rho)$$

measured per processed candidate position (not per message or per dialogue).

Evidence accumulation Each candidate position i maintains an accumulated evidence value $e_i(t)$. When a candidate i first becomes available, a boundary score s_i is computed once using frozen reference windows anchored at that time. This score remains fixed thereafter.

As additional post-boundary context becomes available, evidence is accumulated according to

$$e_i(t+1) = e_i(t) + s_i.$$

This implements a persistence test: a candidate's evidence increases only if the same boundary signal remains present as more context is observed.

Boundary commitment rule At time t , a candidate boundary at position i is committed if and only if

$$e_i(t) \geq \tau(t) \quad \text{and} \quad |i - b| \geq g \quad \forall b \in \mathcal{B},$$

where $\tau(t)$ is the current decision threshold, g is a minimum spacing constraint, and \mathcal{B} is the set of previously committed boundaries. Candidates violating the spacing constraint are suppressed.

Adaptive threshold controller The threshold $\tau(t)$ is updated online to enforce the target selection rate ρ . Let $\hat{\rho}(t)$ denote the empirical selection rate over the most recent W processed candidates (or all candidates if fewer than W have been seen). The controller update is

$$\tau(t+1) \leftarrow \tau(t) + \eta(\hat{\rho}(t) - \rho),$$

where $\eta > 0$ is a step size. Increasing τ reduces boundary commits, while decreasing τ increases them.

Pseudocode The following pseudocode provides a complete operational realization of the adaptive boundary selection procedure described above.

Remarks The adaptive controller operates on candidate positions rather than messages, making the target rate invariant to dialogue length. Evidence accumulation uses a frozen score to test persistence of a boundary signal rather than repeatedly re-scoring shifting contexts. When $\tau(t)$ is held fixed and accumulation is disabled, the procedure reduces to the static selection rule used in the main experiments.

G One-to-one tolerant matching variant for W-F1

Let P be predicted boundaries and G gold boundaries, and let w be the tolerance window. Construct a bipartite graph with edges (p, g) when $|p - g| \leq w$. Compute a maximum-cardinality matching $M \subseteq P \times G$ (ties broken arbitrarily or by minimum total distance). Define $TP = |M|$, $FP = |P| - TP$, and $FN = |G| - TP$, and compute precision/recall/F1 in the usual way. This enforces the one-to-one constraint that each predicted (resp. gold) boundary can be credited at most once.

H Audit protocol and canonicalization details

Controlled We fix: (i) boundary indexing and mapping to turn positions, (ii) the tolerance window w , (iii) metric implementations, and (iv) the operating-point protocol used to select or sweep thresholds to induce a range of BOR values for each method.

Not controlled We do not attempt to replicate each method’s original preprocessing, training regime, or originally reported threshold tuning; therefore, we do not interpret discrepancies with published single-number reports as errors, and we do not attribute differences uniquely to modeling choices independent of preprocessing.

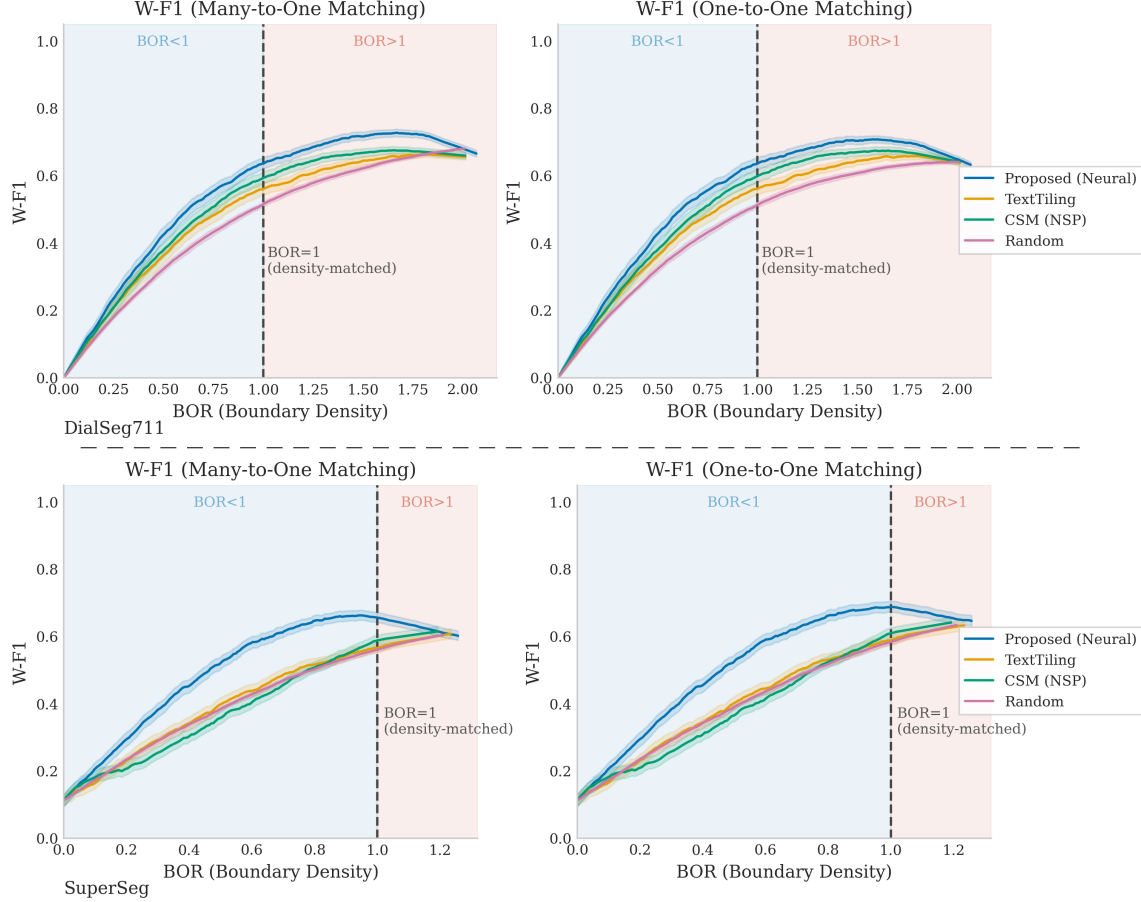


Figure 4: **Robustness of density-quality curves to tolerant matching.** Left: many-to-one (window-coverage) W-F1 used in the main paper. Right: one-to-one tolerant matching via maximum bipartite matching within the same window w . In both datasets, varying boundary density (BOR) induces the dominant changes in W-F1 under either matching, while method differences at matched BOR are secondary. Shaded regions surrounding each curve indicate 95% dialogue-level bootstrap confidence intervals; curves are shown over the full realized BOR range for each dataset under the same threshold sweep. Results reflect the Episodic neural boundary scorer evaluated under static selection and are diagnostic of evaluation behavior rather than full deployed system performance.

References

- Doug Beeferman, Adam Berger, and John Lafferty. Statistical models for text segmentation. *Machine Learning*, 1999.
- Paweł Budzianowski et al. Multiwoz: A large-scale multi-domain wizard-of-oz dataset. In *Proceedings of EMNLP*, 2018.
- Bill Byrne et al. Taskmaster: Toward multimodal, task-oriented dialogue. In *Proceedings of SIGDIAL*, 2019.
- Freddy Y. Y. Choi. Advances in domain independent linear text segmentation. In *Proceedings of NAACL*, 2000.
- Bhavya Chopra, Yasharth Bajpai, Param Biyani, Gustavo Soares, Arjun Radhakrishna, Chris Parnin, and Sumit Gulwani. Exploring interaction patterns for debugging: Enhancing conversational capabilities of ai assistants. *arXiv preprint arXiv:2402.06229*, 2024. URL <https://arxiv.org/abs/2402.06229>.
- Michael H. Coen. Episodic: A conversational memory system. <https://github.com/mhcoen/episodic>, 2025. Accessed 2025-12-12.
- Paul Drew and John Heritage. *Talk at Work: Interaction in Institutional Settings*. Cambridge University Press, Cambridge, UK, 1992.
- Chris Fournier. Evaluating text segmentation using boundary edit distance. In *Proceedings of the 51st Annual Meeting of the Association for Computational Linguistics*, pages 1702–1712, Sofia, Bulgaria, August 2013. Association for Computational Linguistics. URL <https://aclanthology.org/P13-1167/>.
- Chris Fournier and Diana Inkpen. Segmentation similarity and agreement. In *Proceedings of NAACL-HLT*, pages 152–161, Montréal, Canada, June 2012. Association for Computational Linguistics. URL <https://aclanthology.org/N12-1016/>.
- Karthik Gopalakrishnan, Behnam Hedayatnia, Qinlang Chen, Anna Gottardi, Sanjeev Kwatra, Anu Venkatesh, Raefer Gabriel, and Dilek Hakkani-Tür. Topical-chat: Towards knowledge-grounded open-domain conversations. In *Proceedings of Interspeech*, 2019.
- Barbara J. Grosz and Candace L. Sidner. Mixed initiative in dialogue: An investigation into discourse segmentation. In *Proceedings of the 28th Annual Meeting of the Association for Computational Linguistics*, pages 299–306, Pittsburgh, Pennsylvania, 1990. Association for Computational Linguistics. URL <https://aclanthology.org/P90-1010/>.
- Marti A. Hearst. Texttiling: Segmenting text into multi-paragraph subtopic passages. *Computational Linguistics*, 1997.
- Anna Kazantseva and Stan Szpakowicz. Topical segmentation: A study of human performance and a new measure of quality. In *Proceedings of NAACL-HLT*, pages 211–220, Montréal, Canada, June 2012. Association for Computational Linguistics. URL <https://aclanthology.org/N12-1022/>.
- Omri Koshorek, Adir Cohen, Noam Mor, Michael Rotman, and Jonathan Berant. Text segmentation as a supervised learning task. In *Proceedings of NAACL-HLT*, 2018. URL <https://aclanthology.org/N18-2075/>.
- Yanran Li et al. Dailydialog: A manually labelled multi-turn dialogue dataset. In *Proceedings of IJCNLP*, 2020.

- Nelson F. Liu, Kevin Lin, John Hewitt, Ashwin Paranjape, Michele Bevilacqua, Fabio Petroni, and Percy Liang. Lost in the middle: How language models use long contexts. *Transactions of the Association for Computational Linguistics*, 12:157–173, 2024a. doi: 10.1162/tacl_a_00638. URL <https://aclanthology.org/2024.tacl-1.9/>.
- Xiang Liu, Weijia Shi, Yue Zhang, and Philip S. Yu. Dialseg711: A benchmark for dialogue topic segmentation. In *Proceedings of EMNLP*, 2022.
- Xiang Liu, Weijia Shi, Yue Zhang, and Philip S. Yu. Superdialseg: A benchmark for dialogue topic segmentation. In *Proceedings of EMNLP*, 2023.
- Xiang Liu et al. Neural dialogue topic segmentation with contextual representations. In *Findings of the Association for Computational Linguistics*, 2024b.
- Yann Mathet, Antoine Widlöcher, and Jean-Philippe Métivier. The unified and holistic method gamma (γ) for inter-annotator agreement measure and alignment. *Computational Linguistics*, 41(3):437–479, 2015. URL <https://aclanthology.org/J15-3003/>.
- Rebecca J. Passonneau and Diane J. Litman. Discourse segmentation by human and automated means. *Computational Linguistics*, 23(1):103–139, 1997. URL <https://aclanthology.org/J97-1005/>.
- Lev Pevzner and Marti A. Hearst. A critique and improvement of an evaluation metric for text segmentation. *Computational Linguistics*, 2002.
- Amirhossein Razavi, Mina Soltangheis, Negar Arabzadeh, Sara Salamat, Morteza Zihayat, and Ebrahim Bagheri. Benchmarking prompt sensitivity in large language models, 2025. URL <https://arxiv.org/abs/2502.06065>.
- Martin Scaiano and Diana Inkpen. Getting more from segmentation evaluation. In *Proceedings of NAACL-HLT*, pages 362–366, Montréal, Canada, June 2012. Association for Computational Linguistics. URL <https://aclanthology.org/N12-1038/>.
- Melanie Sclar, Yejin Choi, Yulia Tsvetkov, and Alane Suhr. Quantifying language models’ sensitivity to spurious features in prompt design. In *International Conference on Learning Representations*, 2024. doi: 10.48550/arXiv.2310.11324. URL <https://openreview.net/forum?id=RIu5lyNXjT>.
- Hao Sun, Shuangyong Song, and Xiaojun Wan. Topic identification and segmentation in task-oriented dialogue. In *Proceedings of COLING*, 2020.
- C. J. van Rijsbergen. *Information Retrieval*. Butterworths, 2nd edition, 1979.
- Linzi Xing and Giuseppe Carenini. Improving unsupervised dialogue topic segmentation with utterance-pair coherence scoring. In *Proceedings of SIGDIAL*, 2021.
- Wenting Zhao, Xiang Ren, Jack Hessel, Claire Cardie, Yejin Choi, and Yuntian Deng. Wildchat: 1M chatgpt interaction logs in the wild. In *Proceedings of the International Conference on Learning Representations*, 2024.
- Ming Zhong et al. Qmsum: A benchmark for query-based multi-domain meeting summarization. In *Proceedings of NAACL*, 2021.